Case Studies in Construction Materials 16 (2022) e00909

Contents lists available at ScienceDirect

Case Studies in Construction Materials

journal homepage: www.elsevier.com/locate/cscm

Case study

Cracking of residential concrete foundations in eastern Connecticut, USA from oxidation of pyrrhotite

Dipayan Jana

Construction Materials Consultants, Inc. and Applied Petrographic Services, Inc., Greensburg, PA, USA

ARTICLE INFO

Keywords:
Pyrrhotite
Petrography
Microcracking
Microstructure
Ettringite

ABSTRACT

Extensive cracking in thousands of residential foundations in eastern Connecticut is found to be due to expansions from oxidation of pyrrhotite in crushed gneiss coarse aggregate in concrete. Sulfates released from pyrrhotite oxidation reacted with aluminous phases in paste to cause internal sulfate attacks and further expansions. These two-stage expansion processes took as long as 15 years of service in the presence of oxygen and moisture to develop extensive cracking to crumbling. The unsound pyrrhotite-bearing quartz-feldspar-biotite-garnet gneiss of Ordovician Brimfield Schist formation came from a quarry on a hydrothermal vein of significant pyrrhotite crystallization. Microstructural, chemical, and mineralogical evidences of pyrrhotite oxidation and resultant internal sulfate attack are presented from a residential concrete foundation in Mansfield, Connecticut. Ferrihydrite oxidation product of pyrrhotite, bands of oxidized iron in iron sulfide bodies, and microcrystalline fibrous secondary ettringite deposits intermixed with the cement hydration products in paste as well as deposited in cracks, voids, and porous areas of paste are the products of two-stage expansions that have contributed to the distress. Occurrences of numerous pyrrhotite bearing metamorphic rocks of the Appalachian mountains along eastern US pose concerns of similar distress of many homes with urgent need for standardized testing protocols to control pyrrhotite-related distress. A five-stage testing protocol is proposed to screen potentially deleterious pyrrhotite-bearing aggregates for mitigating this distress in future constructions.

1. Introduction

Widespread cracking and crumbling of many residential concrete foundations have occurred in the eastern United States of Connecticut and Massachusetts due to oxidation of an iron sulfide mineral, pyrrhotite, in the quarried coarse aggregate stones with over 35,000 homes in CT and over 10,000 homes in MA being affected. Pyrrhotite (from Greek *pyrrhos* i.e. flame-colored or redness) commonly occurs in many mafic igneous, sedimentary, and metamorphic rocks, or in high temperature hydrothermal and replacement veins as a minor accessory mineral having a chemical formula of $Fe_{1-x}S$, where x varies from 0 to 0.125. It is commonly associated with pyrite (FeS_2) but is distinguished by its bronze rather than brass color of pyrite, its lower hardness, decomposition in HCl (Deer et al. [1]), lower S/Fe ratio, and weakly magnetic nature. All these features along with X-ray diffraction of rocks containing both iron sulfide minerals help to determine the pyrrhotite content, whereas XRF or infrared combustion analysis of rocks determine the sulfur contents from all iron sulfide minerals. Pyrrhotite has four times higher solubility and a much faster rate of oxidation in the presence of oxygen and moisture than its closest ally, pyrite, which makes pyrrhotite a more serious candidate for oxidation-related distress in concrete

E-mail address: info@cmc-concrete.com.

https://doi.org/10.1016/j.cscm.2022.e00909
Received 29 September 2021; Received in revised form 23 December 2021; Accepted 21 January 2022
Available online 22 January 2022

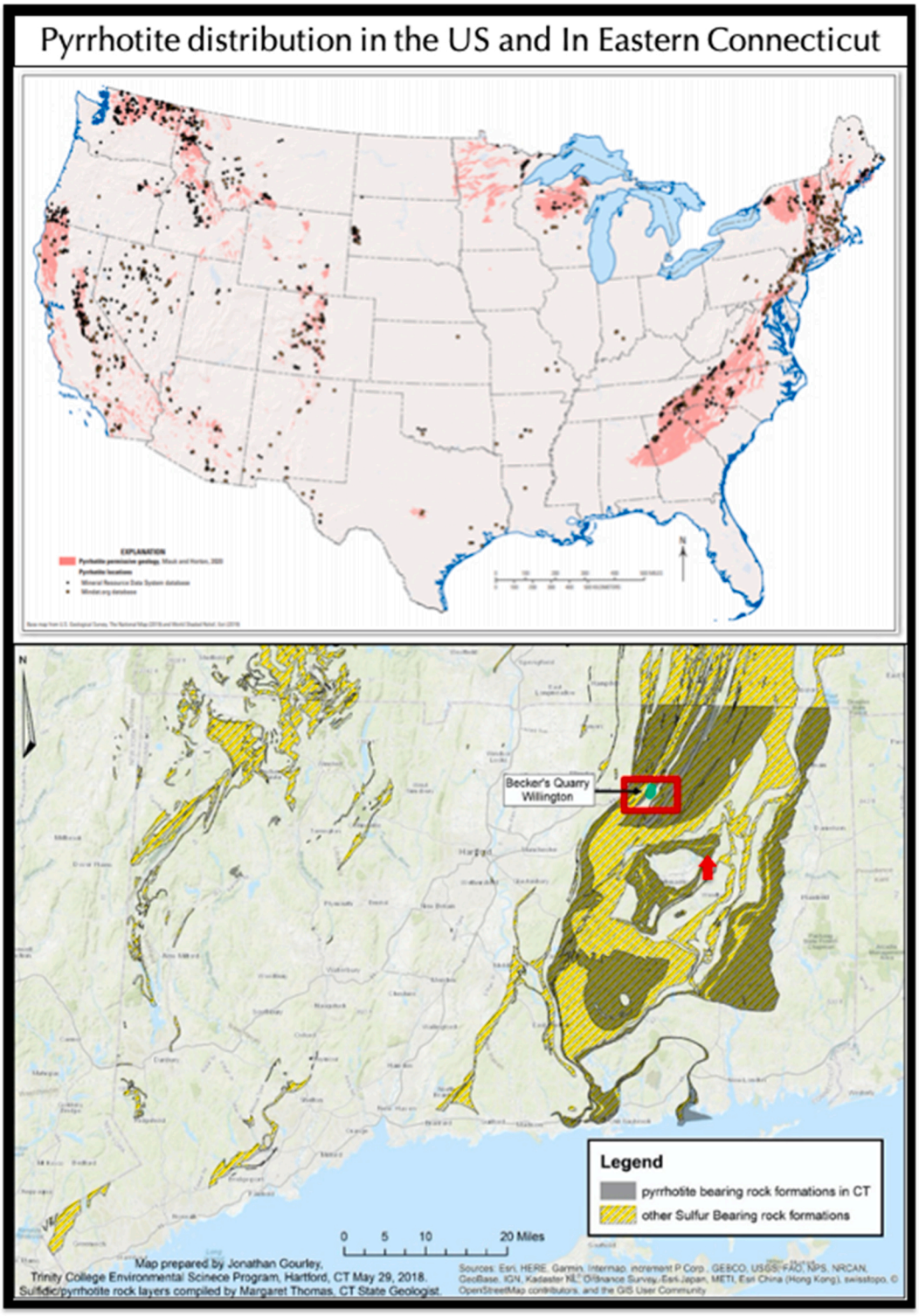

Fig. 1. Maps showing potential distribution of pyrrhotite across the continental US as black dots in the top map [23], and, in the eastern Connecticut region as dark shaded areas in the bottom map [24]. The top map prepared by USGS shows a narrow elongated belt of potential pyrrhotite crystallization in the metamorphic rocks of the Appalachian mountains along the east coast. The square in the bottom map shows location of the Becker's quarry, which supplied the coarse aggregates for concretes in the entire shaded areas showing pyrrhotite-oxidation related distress. The red arrow shows the location for this case study.

than pyrite.

Although most of the information available on pyrrhotite-related concrete deterioration in northeastern Connecticut is presently limited to news media, the cause of deterioration has been investigated in laboratories by Wille and Zhang [2], Zhang and Wille [3], and Jana [4]. Similar distresses from pyrrhotite oxidation have been reported from Norway [5], Canada [6–9], and Pyrenees, Spain [10–14]. Similar distresses from oxidation of pyrite have been reported from Canada [15–18], Wales [19], and USA [20–22].

In all these studies, the deterioration is attributed to oxidation of pyrrhotite (or pyrite) present in the concrete aggregates in the presence of moisture and oxygen during service. Most studies proposed two-stage expansions due to (a) oxidation of pyrrhotite (or pyrite) in the presence of oxygen, moisture, and high pH in concrete to form various forms of ferric oxy-hydroxides, e.g., goethite [FeO(OH)], ferrihydrite [$Fe(OH)_3$] etc. causing cracking of the unsound aggregates, which is followed by (b) internal sulfate attacks by the sulfates released from oxidation of iron sulfide grains forming gypsum, ettringite, and/or thaumasite. The former expansion is contributed from the volume increase from oxidation of iron sulfides to iron oxy-hydroxides, whereas, the latter expansion is contributed from volume increase due to formation of various hydrates of calcium or sodium sulfates (gypsum, thenardite, mirabilite), calcium sulfoaluminate (ettringite), or, calcium silico-sulfate-carbonate (thaumasite) in the confined areas in paste. Manifestation of the damage for pyrrhotite-oxidation cases has taken as many as 10–20 years to develop serious cracking.

Typical visual deterioration is in the form of map cracking, pop outs of near-surface unsound pyrrhotite-containing aggregates, reddish-brown discoloration as rust stains from leaching of iron oxy-hydroxides, whitish formation of efflorescence salts of sulfates (thenardite, mirabilite, gypsum, ettringite, thaumasite), and carbonates (calcite, aragonite) in the vicinity of surface cracking, and, in severe cases as found in many homes in eastern Connecticut deformation and crumbling of concrete.

2. Scope of work

In Connecticut and Massachusetts, most of the damages of residential concrete foundations have been linked to crushed stones supplied during 1983 through 2015 from one square-shaped quarry (Becker's quarry) located in Willington, CT that sits in a weathered hydrothermal vein of metamorphic rocks containing significant pyrrhotite mineralization. The geology in the vicinity of the quarry is made up of metamorphic rocks mapped as Ordovician Brimfield Schist consisting predominantly of gray, rusty brown to orange-yellow weathered, medium to coarse grained, interlayered foliated schist and gneiss, granofels, and foliated quartz diorite. Quartz, plagioclase or oligoclase are primary minerals with micas, and noted are garnet and pyrrhotite as common accessory minerals. A recent map of potential distribution of pyrrhotite in the continental US compiled by United States Geological Survey [23] showed intense localization along a narrow elongated belt following the Appalachian mountains in the eastern US, and some isolated patches in the Western US. Fig. 1 shows potential distribution of pyrrhotite in the US, and in eastern Connecticut [23,24].

In light of this known problem of pyrrhotite oxidation and resultant distress, and its discovery in the crushed gneiss coarse aggregate particles in many residential foundations in northeastern Connecticut, which were all reportedly quarried from the Becker's quarry in CT, the present investigation focused on one severely cracked residential foundation located in Mansfield, Connecticut, which is situated within the known area of 'pyrrhotite epidemic.' The study revolved around investigating the role of pyrrhotite from its abundance to the mechanism of deterioration. Field photographs of the subject foundation walls showed extensive cracking (Fig. 2) as a network of closed polygonal-shaped cracks. Concrete cores were drilled over visible cracks from the interior walls of the foundation and drilled through the entire wall thickness (Fig. 2).

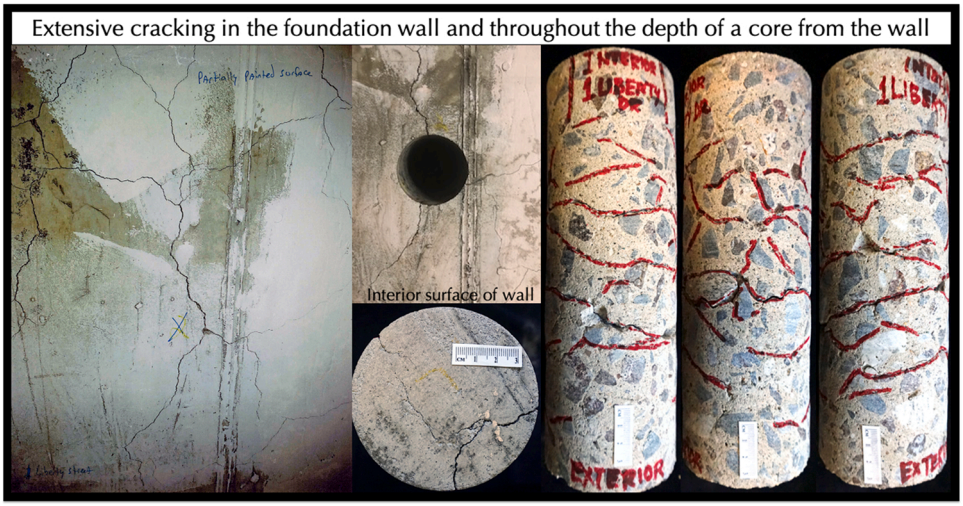

Fig. 2. Cracking of a residential concrete foundation in the eastern Connecticut shown in the leftmost photo, which is the subject of this study. A core retrieved from over a visible crack in the foundation wall showed extensive cracking through the entire recovered length from the interior to the exterior surface of the wall, many of which are highlighted in red on the cylindrical surface.

3. Methodologies

Laboratory investigations were conducted to determine the presence of oxidized pyrrhotite in concrete first by detailed petrographic examinations (optical microscopy) according to the procedures of ASTM C 856 [25] from: (a) visual examinations of cores received to determine the extent of cracking (Fig. 2) and detection of the abundance and distribution of potentially unsound pyrrhotite-bearing coarse aggregates, (b) scanning of saw-cut, polished, and fluorescent-epoxy-impregnated lapped cross sections of core on a flatbed scanner to determine the abundance and distribution of pyrrhotite aggregates and the extent of cracking (Fig. 3), (c) stereo-microscopical examinations of polished cross sections of cores to detect occurrences of 'oxidized' pyrrhotite grains from the characteristic fine striations and reddish-brown oxidation products (Fig. 4), (d) UV light observations of fluorescent epoxy-impregnated lapped sections in a dark room and with a stereo-microscope to determine the extent of cracking, and from (e) examinations of blue dye-mixed epoxy-impregnated thin sections of concrete in a petrographic microscope to detect the unsound aggregates (Fig. 5), and microstructures of pyrrhotite-oxidation-related distress from macro and microcracking to oxidation products to results of sulfate attack in paste (Figs. 6–9) from the sulfates released from pyrrhotite oxidation.

Following optical microscopy, an in-depth examination of oxidation products of pyrrhotite and compositional and microstructural investigations of affected paste fractions are done on multiple thin sections in a scanning electron microscope equipped with secondary electron and backscatter electron detectors and energy-dispersive X-ray spectrometer (SEM-EDS) by following the procedures of ASTM

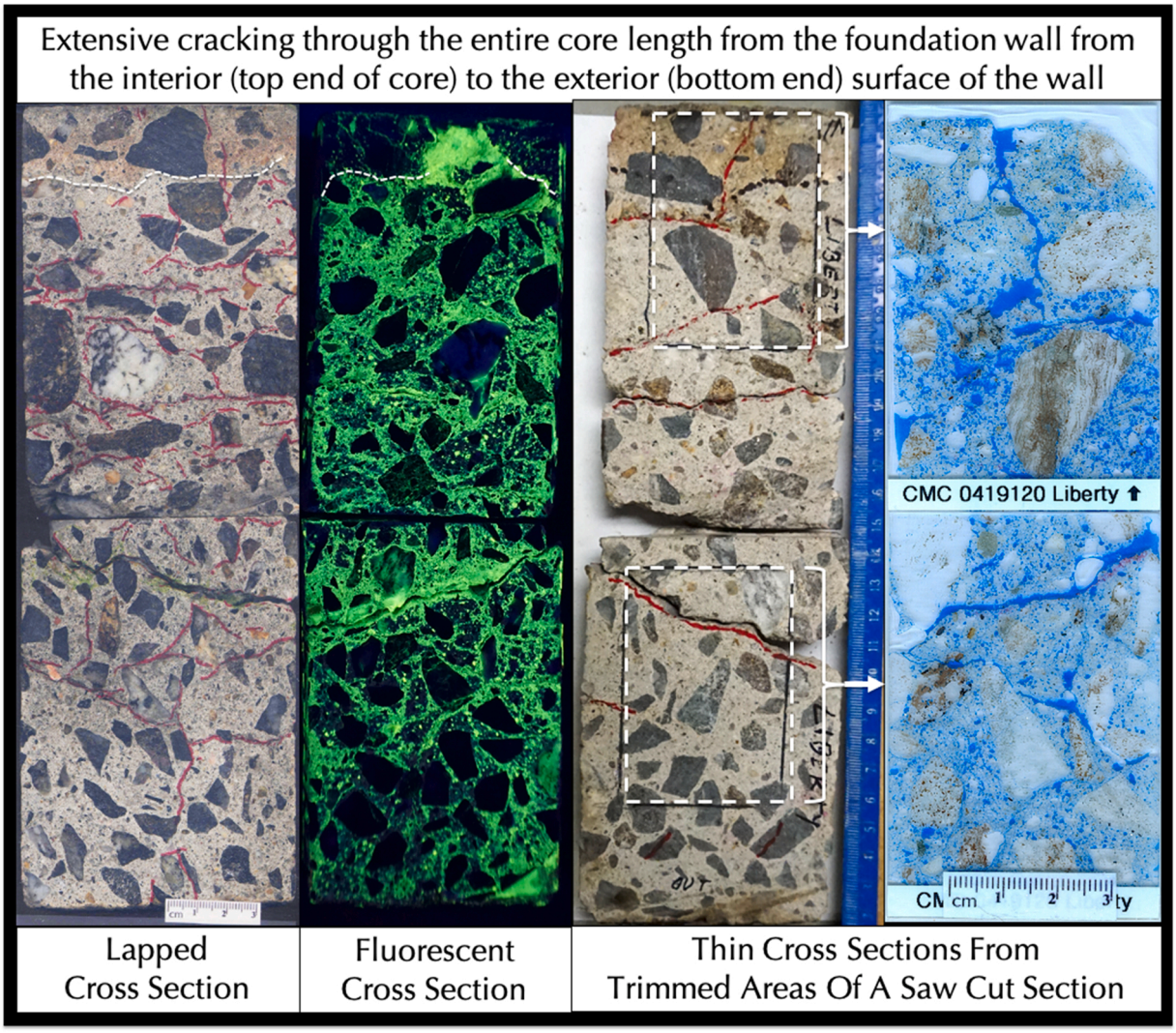

Fig. 3. From left to right: (a) lapped cross section of core where extensive cracks are marked in red and depth of carbonation from interior wall surface is marked in white dashed line at the top; (b) fluorescent epoxy impregnated lapped cross section seen in an UV light where carbonated zone is dark due to densification of paste, aggregates are also dark due to dense natures, whereas cracks are highlighted; (c) two saw-cut sections selected from both ends of the core for preparation of blue dye-mixed epoxy-impregnated thin sections, which are shown in the rightmost photo, where (d) cracks are highlighted in blue epoxy.

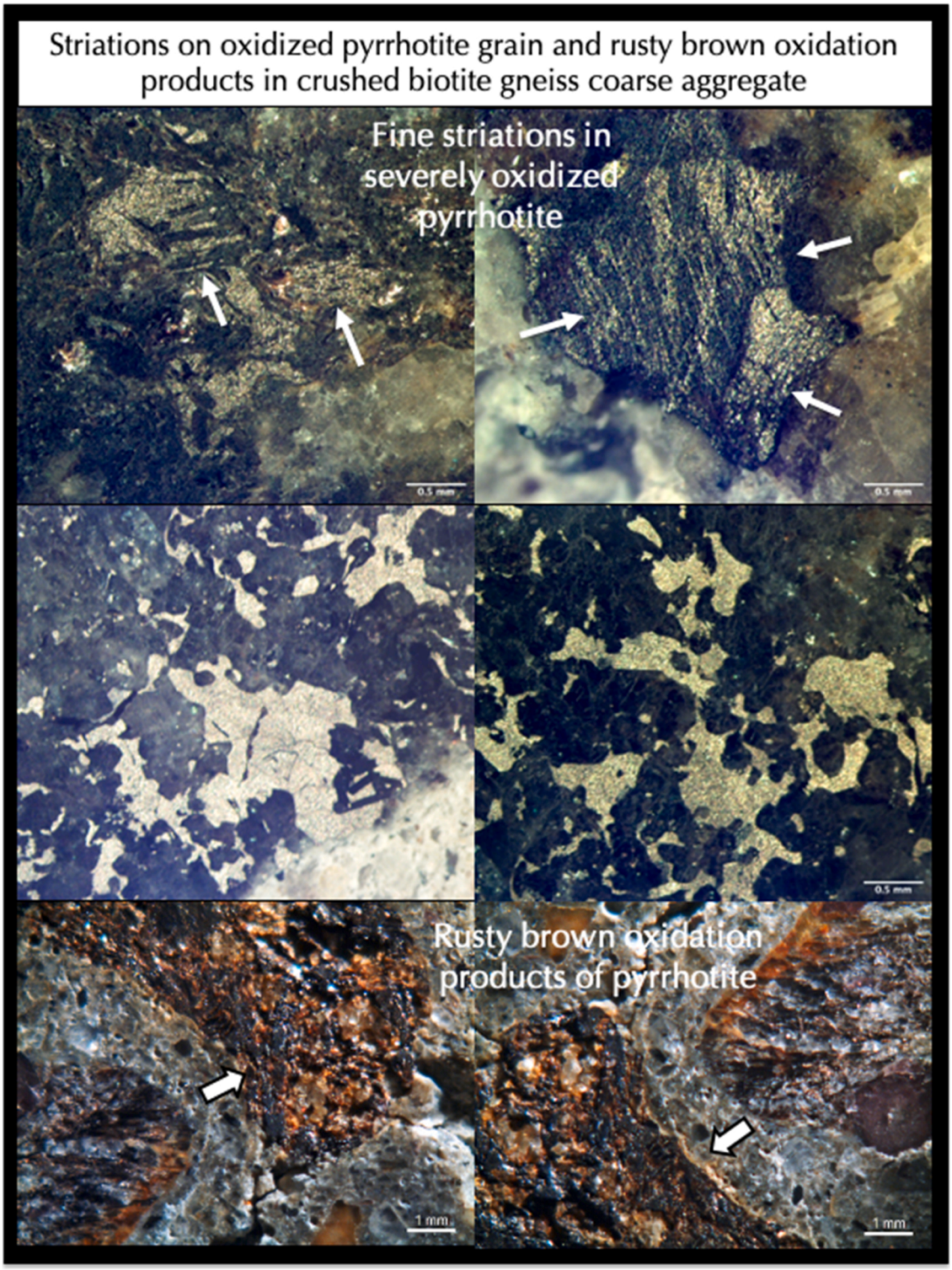

Fig. 4. Micrographs of polished cross section of a core showing: (a) fine striations of oxidized iron in pyrrhotite grains in coarse aggregate, many of which are marked with arrows oriented perpendicular to the striations in the top row, whereas (b) lack of such distinct striations in non (or less)-oxidized pyrrhotite grains (middle row), and (c) rusty brown oxidation products of pyrrhotite in severely cracked aggregates (bottom row).

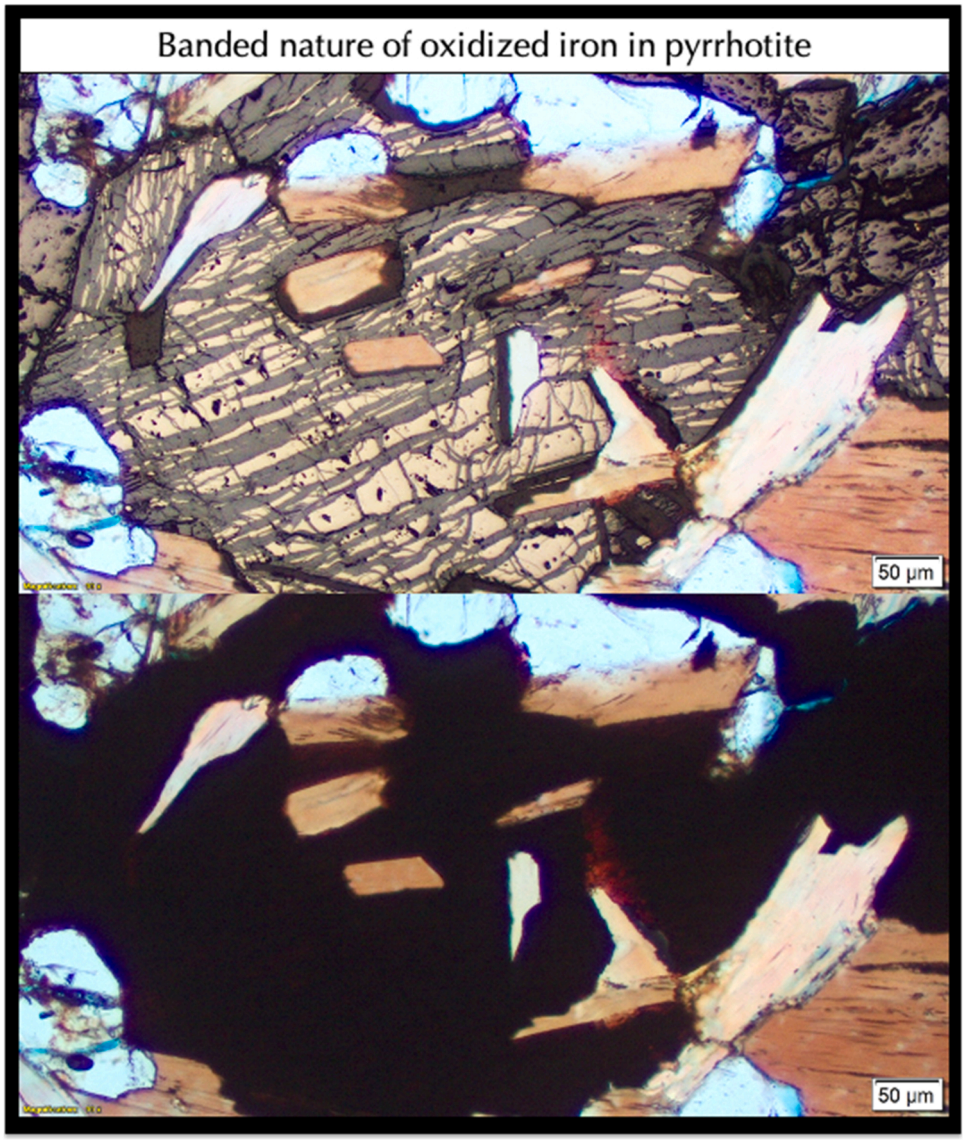

Fig. 5. Micrographs of thin section of a core showing fine gray striations in an oxidized pyrrhotite grain in crushed gneiss coarse aggregate, where iron oxide bands appear as medium gray against brighter iron sulfide body in reflected and transmitted polarized light (top row), as opposed to dark opaque appearance of the entire oxidized pyrrhotite grain in transmitted polarized light (bottom row). Pyrrhotite grains are commonly associated with and sometimes engulf many biotite flakes as seen here.

C 1723 [26]. SEM-EDS studies determined compositional variations of oxidized iron veins in pyrrhotite grains (Figs. 10 and 11) and composition and microstructure of affected paste (Fig. 12).

Following petrographic examinations, multiple pyrrhotite-bearing coarse aggregate particles were extracted from the concretes for X-ray diffraction (XRD, according to ASTM C 1365 [27]), X-ray fluorescence (XRF), and ion chromatography (IC, according to ASTM D 4327 [28]). Thin slices of core through the entire depth (i.e., of wall thickness) were also extracted for XRD, XRF, and IC of bulk concrete. Seven pyrrhotite-bearing aggregates were extracted from the core, which along with the thin slice of concrete were pulverized down to finer than 44 μm (US 325 sieve) size and pressed into 32 mm pellets with a 25-ton hydraulic pellet press for XRD and XRF analyses (Fig. 13). Unsound aggregates were also selectively drilled with a benchtop drill press from the polished cross sections of core where drill dusts were analyzed on a zero background plate in XRD for detection of pyrrhotite and its oxidation products. For IC, extracted aggregate particles and concrete were digested in a strong oxidant of 35% hydrogen peroxide solution for several days in an accelerated oxidation test [2,29], and then diluted in distilled water to determine the levels of sulfates released by these aggregates in relation to a 'control aggregate' without any iron sulfide mineral (Fig. 14).

Instruments used are digital camera and Epson flatbed film scanner for photographs of core and cross/thin sections of core, respectively, Buehler Petrothin and Ecomet for thin sectioning and lapping, respectively, Nikon Eclipse E600 POL petrographic

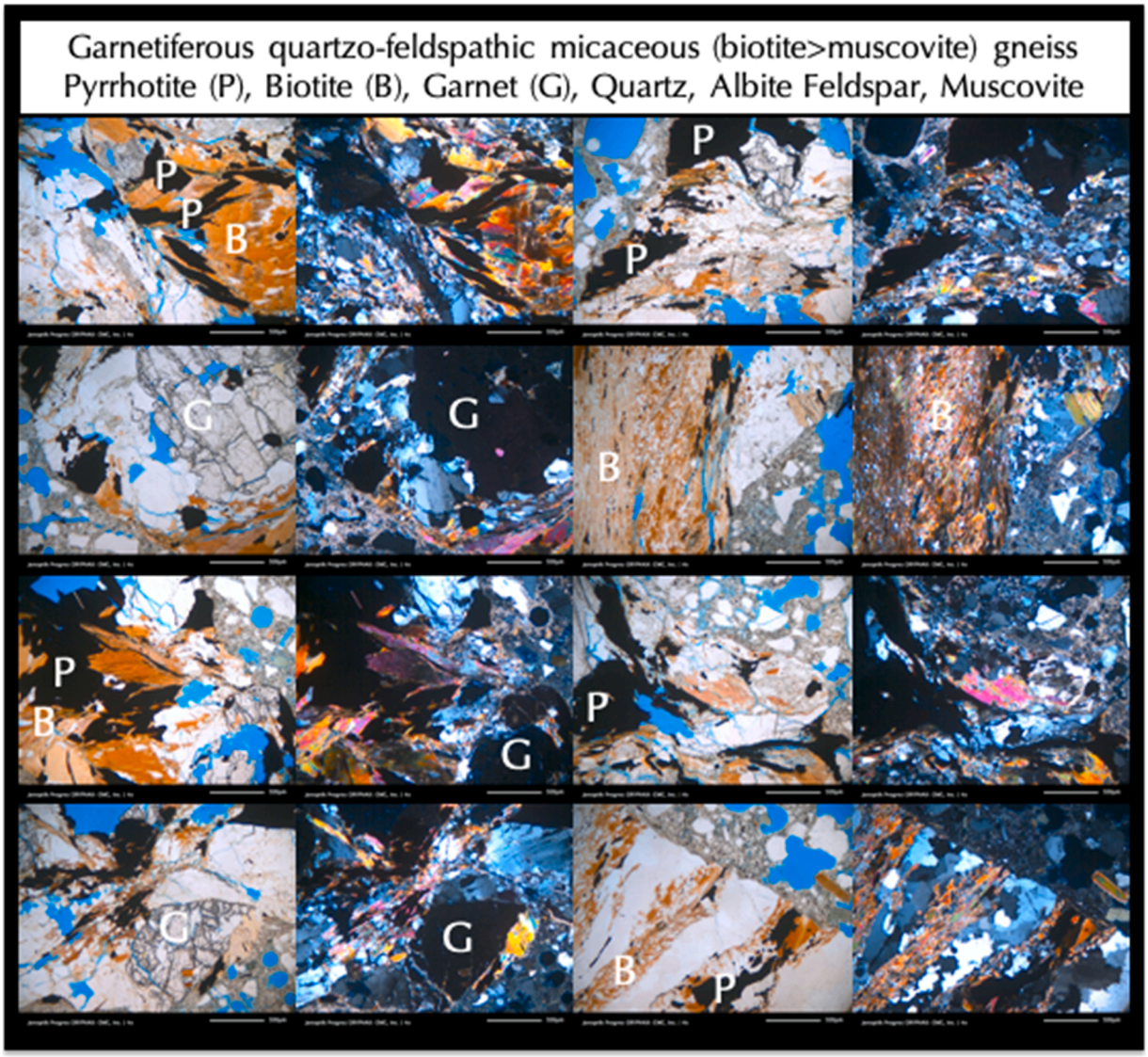

Fig. 6. Micrographs of blue dye-mixed epoxy-impregnated thin sections of concrete showing crushed quartz-feldspar-biotite (B)-garnet (G)-pyrrhotite (P) bearing crushed schist and gneiss coarse aggregate particles, parallel alignment of quartzo-feldspathic and micaceous minerals, often arranged in alternating bands characteristic of gneissose textures. Pyrrhotite (P) grains occur as dark opaque inclusions in these photos, many of which show bands of oxidized iron in sulfide bodies when viewed through reflected and transmitted polarized lights as shown in Fig. 5. Scale bars are 0.5 mm.

microscope with transmitted plane and crossed polarized light, reflected (metallurgical) observations of pyrrhotite grains in polished samples, and fluorescent light facilities for highlighting macro and microcracks, CamScan Series II SEM with SE, BSE, and EDS detectors for compositional and microstructural analyses of oxidized pyrrhotite and affected mortar fractions, Siemens D5000 and Bruker D2 Phaser for mineralogical analyses by XRD, Rigaku NEX-CG for bulk oxide (sulfate) contents of aggregates and concrete by ED-XRF, and Metrohm 881 IC with attached 868 auto sample changer for water-soluble sulfate contents released from aggregates and concrete after accelerated oxidation.

4. Results

4.1. Optical microscopy

Petrographic examinations detected crushed gneiss coarse aggregate as the host rock for pyrrhotite, where pyrrhotite grains occur as fine disseminated dark opaque accessory iron sulfide grains mixed with quartz, potash feldspar (oligoclase), albite (plagioclase), biotite mica, and garnet. Fig. 4 shows fine striations of oxidized veins in oxidized pyrrhotite grains whereas lack of such striations in

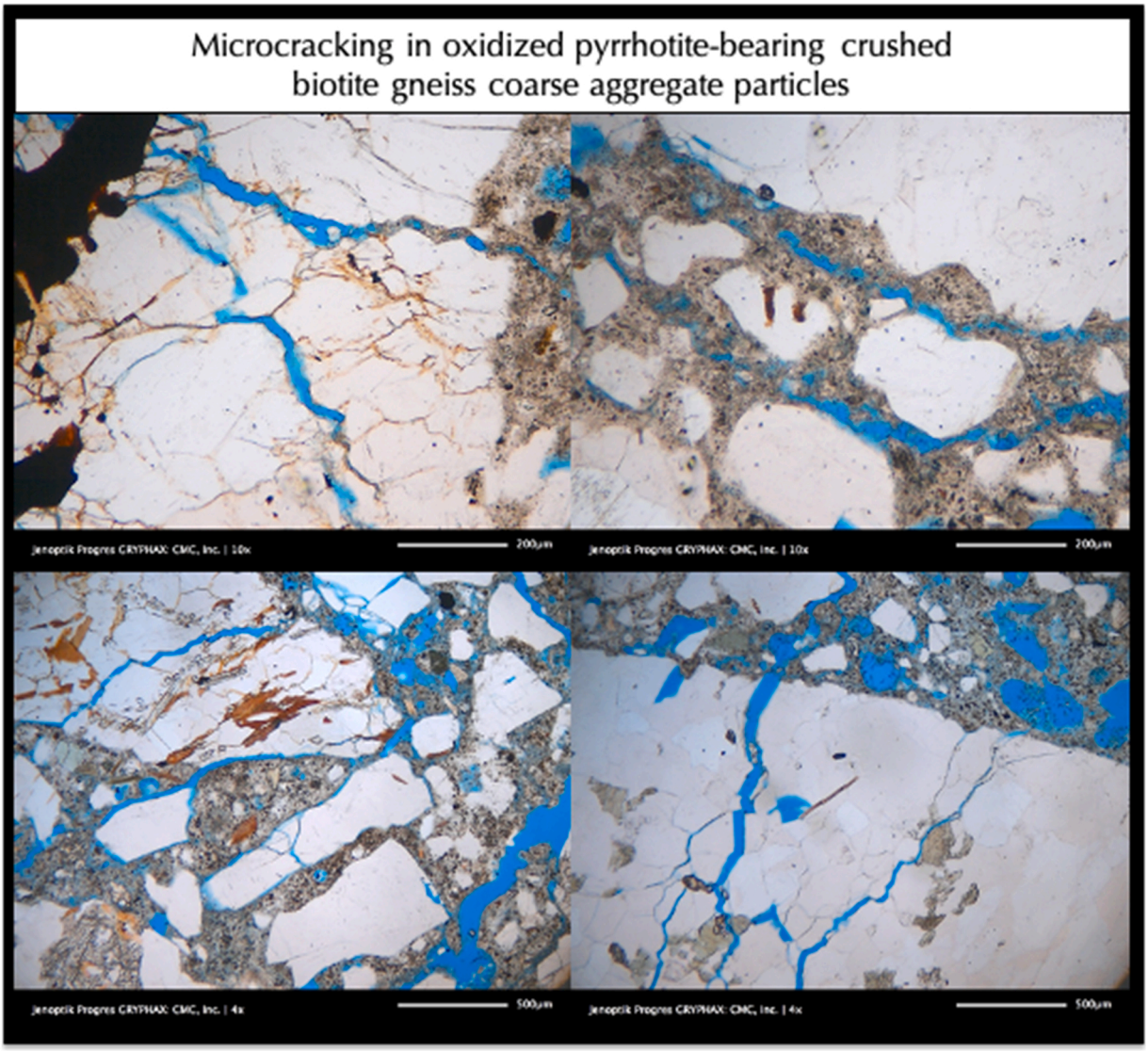

Fig. 7. Micrographs of blue dye-mixed epoxy-impregnated thin sections of concrete showing extensive microcracking in unsound pyrrhotite grains often extending into paste. Scale bars are 0.2 mm (top row) and 0.5 mm (bottom row).

non (or less) oxidized pyrrhotite grains on lapped cross sections of core viewed through a stereomicroscope. Fig. 5 shows distinct bands of oxidized iron in pyrrhotite body in a thin section viewed through both reflected and transmitted polarized light, as opposed to dark opaque appearance of both oxidized and sulfide phases in the grain when viewed only through transmitted polarized light. Thin sections show typical schistose textures of parallel alignment of quartz, feldspar, and biotite grains, or, in alternating bands of quartzo-feldspathic and micaceous minerals in gneissose textures (Fig. 6). The mineralogy, texture, and host rock type are similar to many other foundations from the area where unsound pyrrhotite-bearing aggregates were quarried from the hydrothermal vein in Becker's quarry situated in Willington, CT.

Petrographic examinations determined the overall concrete compositions containing: (a) crushed gneiss coarse aggregate having a nominal maximum size of 19 mm, (b) natural siliceous sand fine aggregate having a nominal maximum size of 9.5 mm (containing major amounts of quartz and quartzite, and subordinate amounts of feldspar, mica, ferruginous rock, and mafic minerals); (c) hardened Portland cement paste having a cement content estimated to be 6–$6^{1}/_{2}$ bags per cubic yard, and a water-cement ratio (w/c) estimated to be 0.45–0.50, and (d) an air content estimated to be 6–8% with an indication of use of an air-entrained concrete.

Petrographic examinations detected mixtures of three different color tones of coarse aggregate particles: (a) dominant dark gray to black gneiss consisting of parallel alignment of quartz, albite feldspar, biotite mica, and occasional pyrope garnet porphyroblasts, anhedral to subhedral equigranular to gneissose arrangement of minerals; (b) subordinate light to medium brown granite gneiss of quartz, albite feldspar, garnet, biotite mica and occasional pyroxene (augite) grains; and (c) minor white granite gneiss with quartzo-feldspathic minerals and black specs of mica flakes in parallel alternate (gneissose) arrangements. Brown and dark gray gneiss contain

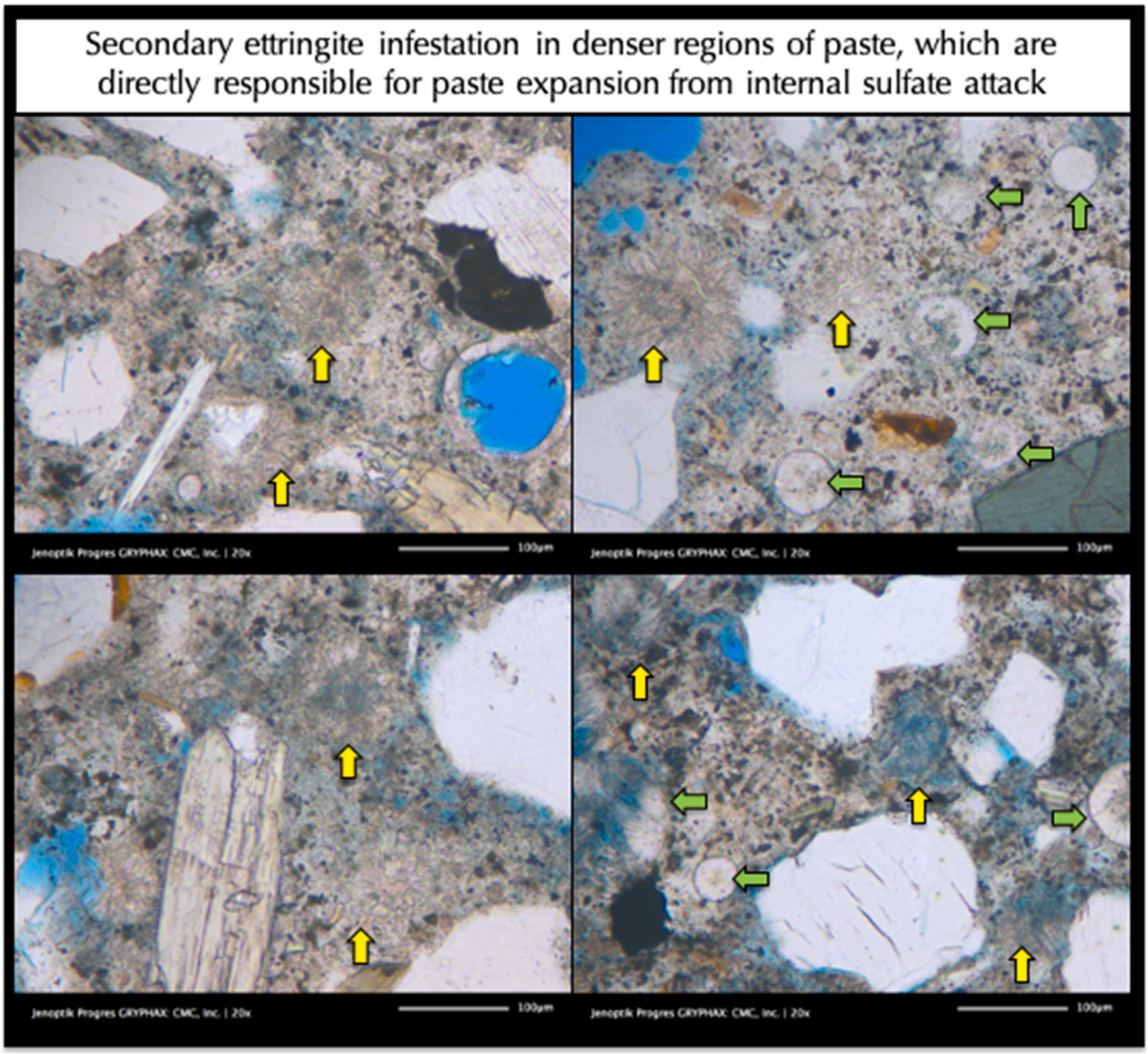

Fig. 8. Micrographs of blue dye-mixed epoxy-impregnated thin sections of concrete showing potentially deleterious ettringite infestation in paste, many of which are marked with yellow arrows. Green arrows show ettringite precipitations in relatively open spaces as porous regions of paste and in air voids. Scale bars are 0.1 mm.

more iron sulfide and iron oxide minerals than the minor white granite gneiss. All particles are angular, dense, hard, and medium to dark gray to brown, gneissose-textured, equidimensional to elongated, variably altered, uncoated, and variably cracked. Coarse aggregate particles are well-graded and well-distributed. There is no evidence of alkali-aggregate reactions of coarse aggregates in concrete.

Similar to the predominant dark gray to brown pyrrhotite-bearing gneiss that have caused pyrrhotite oxidation and subsequent distress in other case studies, present study also showed the dark gray to brown unsound pyrrhotite-bearing garnetiferous quartzo-feldspathic gneiss particles compared to the lighter colored (white with black specs of mica) granite gneiss that contained the disseminated unsound pyrrhotite grains to cause extensive micro and macrocracking (Fig. 7).

Paste fractions showed profuse development of secondary ettringite in cracks, microcracks, voids, and pore spaces (Figs. 8 and 9) due to the presence of moisture and released sulfates from pyrrhotite oxidation. Ettringite infestation in paste has produced the telltale evidence of sulfate release and related distress from pyrrhotite oxidation.

4.2. SEM-EDS studies

The most characteristic compositional and microstructural evidence of pyrrhotite oxidation revealed from SEM-EDS studies is the oxidized bands or veins of iron in pyrrhotite grains where the veins appear in darker shades of gray in BSE and SE images compared to

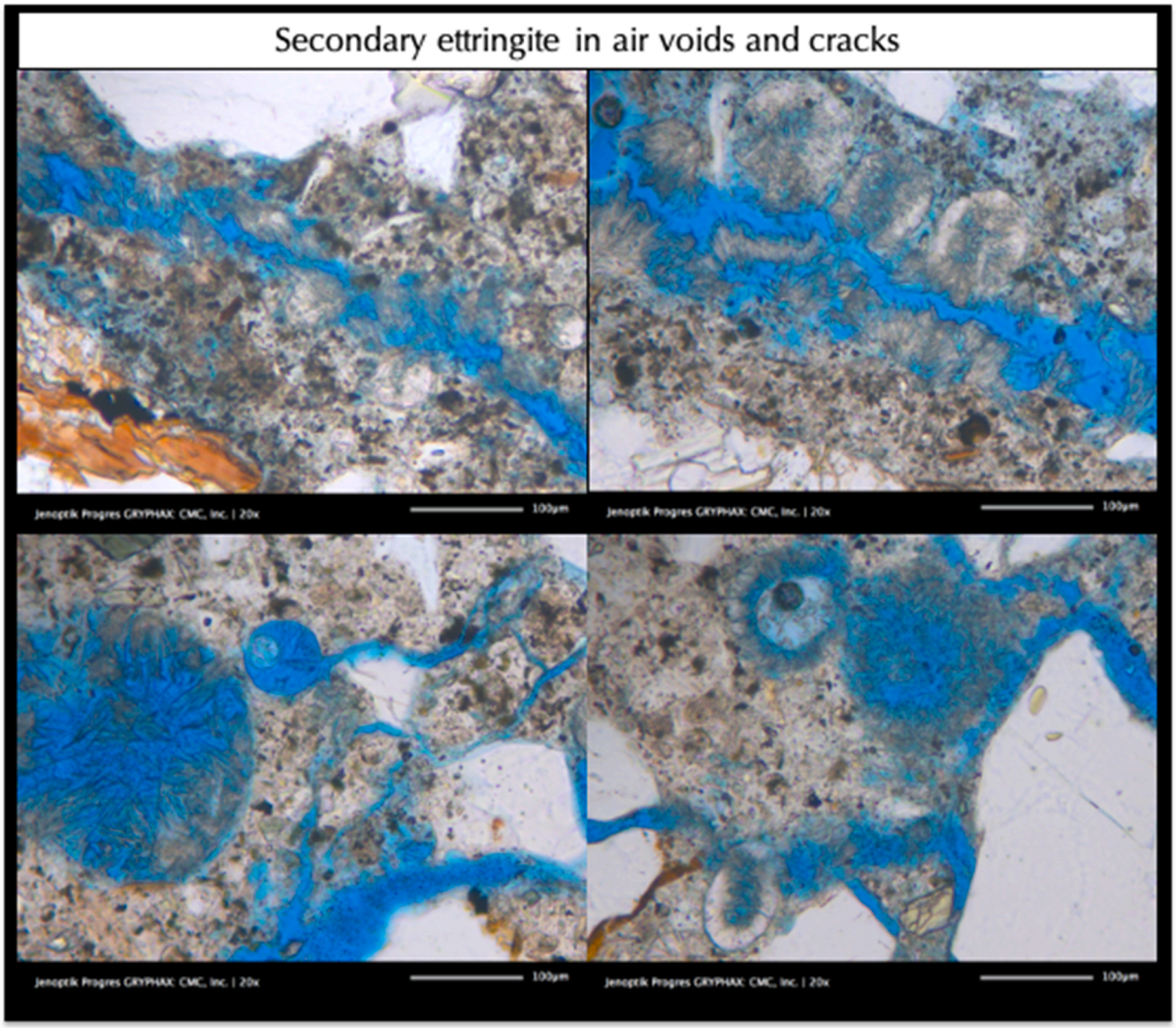

Fig. 9. Micrographs of blue dye-mixed epoxy-impregnated thin sections of concrete showing ettringite infestation in cracks and voids. Scale bars are 0.1 mm.

the brighter iron sulfide bodies (Figs. 10 and 11). Compositional and X-ray elemental analysis of pyrrhotite show iron and oxygen enrichment of oxidized veins (as > 95%FeO) as compared to iron and sulfur enrichment of pyrrhotite bodies (as 60–65% FeO and 30–35% SO_3). The interstitial mortar fractions show many typical features of pyrrhotite distress, e.g., microcracking, profuse development of secondary ettringite in cracks, voids, and porous areas of paste, and ettringite infestations in denser regions where fine fibrous ettringite is intermixed with cement hydration products (Fig. 12).

SEM-EDS studies showed: (a) evidence of secondary ettringite crystallization in cracks and gaps along aggregate-paste interfaces (Fig. 12); (b) secondary ettringite crystallization in air-voids (Fig. 12); (c) sulfate contamination of paste from released sulfates from oxidation of pyrrhotite in coarse aggregates (Fig. 12); (d) occasional gaps around coarse aggregates due to expansion of sulfate-contaminated paste; (e) evidence of fine disseminated iron sulfide inclusions in quarried aggregates, having lower S/Fe atomic ratios than pyrite to indicate their pyrrhotite compositions (Fig. 10); (f) evidence of oxidation of pyrrhotite and formation of iron oxide veins within pyrrhotite (Figs. 10 and 11); (g) evidence of unsoundness of pyrrhotite-bearing aggregate from expansion and cracking; and (h) secondary ettringite infestation in confined areas in paste. All these microstructural features are characteristic of pyrrhotite-oxidation related distress, which are also found in many other foundations from the area.

4.3. X-ray diffraction

XRD analyses of seven different dark gray and brown coarse aggregate particles extracted from the core as well as XRD analysis of the bulk concrete sliced from the entire length of the core showed mineralogical similarities to concretes from many other distressed foundations, including the absence of any detectable pyrrhotite in XRD (despite its detection in optical microscopy and SEM-EDS) but

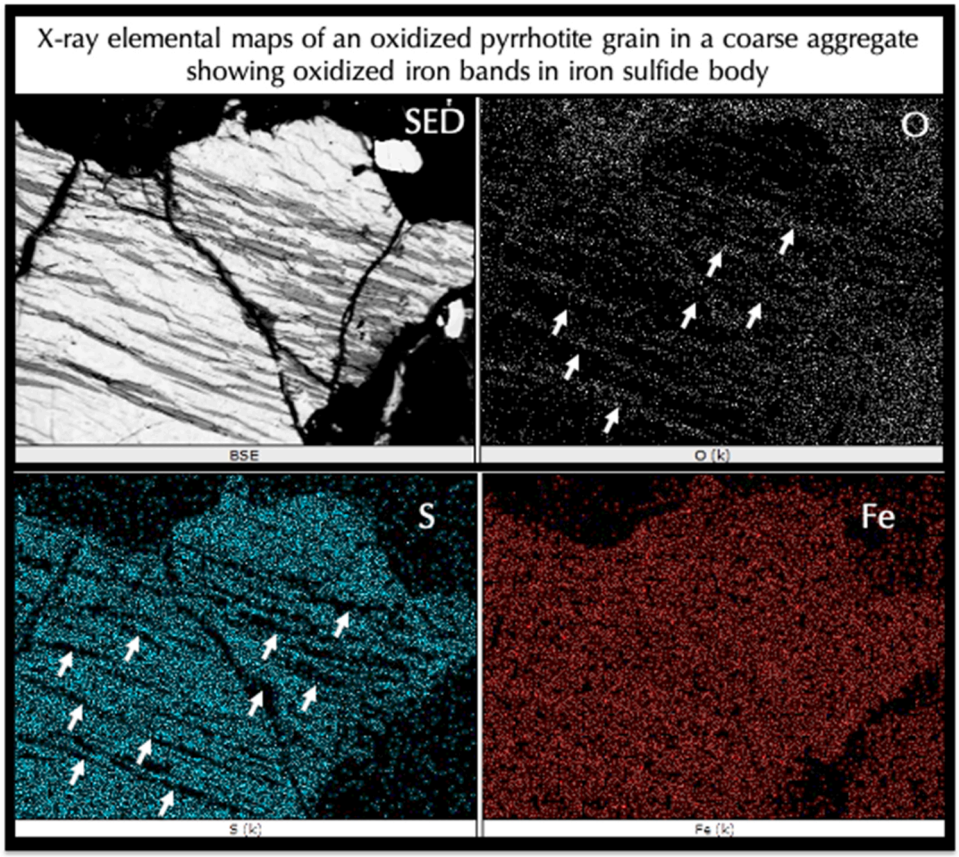

Fig. 10. Backscatter electron image (top left) and corresponding X-ray elemental maps of Fe, S, and O in an oxidized pyrrhotite grain showing veins of oxidized iron appearing as gray bands in BSE image within the brighter pyrrhotite body that are highlighted by iron (Fe) and oxygen (O) maps for oxidized iron veins (arrows), Fe and S maps for interstitial non-oxidized sulfide matrix of pyrrhotite. Field width is 1.4 mm.

the presence of ferrihydrite type iron hydroxide phase (Fig. 13). Oxidation of pyrrhotite to ferrihydrite released sulfates, which have caused formation of ettringite in cracks, voids, and paste to be detected in XRD analyses of many extracted aggregates.

4.4. X-ray fluorescence

XRF studies of dark gray and brown crushed gneiss coarse aggregates showed variable sulfate contents, probably due to variable pyrrhotite contents in these particles but the bulk concrete showed noticeable sulfate (2.37% as SO_3), which is noticeably higher than the amount contributed from Portland cement as the sole source of sulfate (for a concrete having 15% Portland cement by mass and 3% sulfate in cement, cement's SO_3 contribution to concrete is 0.45%). This additional sulfate is released from the oxidation of pyrrhotite.

4.5. Accelerated oxidation tests

In accelerated pyrrhotite oxidation test [2,29], seven crushed gneiss coarse aggregate particles were extracted from the core, cleaned of adhered paste remains, crushed, then immersed in a 35% hydrogen peroxide (strong oxidant) solution for 10 days. Sulfates released from aggregates to the filtrates were measured (as SO_4^{-2}) in an anion exchange chromatograph. All particles showed noticeable release of sulfates from aggregates and concretes as opposed to no sulfate release from a control gneiss aggregate containing no pyrrhotite indicating the potential for continued sulfate release in the field during service in prolonged presence of moisture (Fig. 14).

4.6. Microcracking

Following the field evidence of distress from map cracking of foundation walls, extensive microcracking of many unsound pyrrhotite-bearing coarse aggregate particles causing fine striations to be detected on polished sections during stereo-microscopical observations, or in thin sections during observations in a petrographic microscope, along with detection of extension of cracking into the mortar fractions are the first telltale evidence of pyrrhotite-oxidation related distress in concrete. Cracks are best revealed on

Compositional analyses of an oxidized pyrrhotite grain in a coarse aggregate from oxidized veins and interstitial sulfide dody

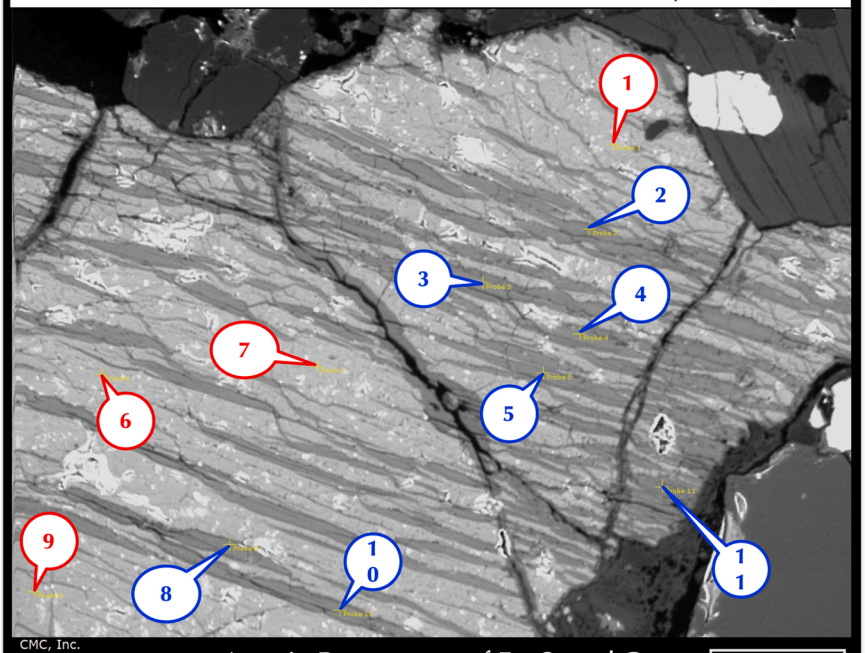

CMC, Inc.
20.0 KV EM Mag 200X
Captured by Dipayan Jana

Atomic Percentages of Fe, S, and O

200nm

Probe	O	Fe	S	S/Fe	O/Fe	O	Fe	S	S/Fe	O/Fe	Phase
1	0.00	35.21	66.81	1.90	0.00	0.00	35.21	66.81	1.43	0.00	Pyrrhotite
2	27.55	65.38	0.00	0.00	0.42	27.55	65.38	0.00	0.00	0.42	Iron Oxide
3	24.81	66.20	0.00	0.00	0.37	24.81	66.20	0.00	0.00	0.37	Iron Oxide
4	28.32	65.15	0.00	0.00	0.43	28.32	65.15	0.00	0.00	0.43	Iron Oxide
5	30.35	64.55	0.00	0.00	0.47	30.35	64.55	0.00	0.00	0.47	Iron Oxide
6	2.35	35.05	65.88	1.88	0.07	2.35	35.05	65.88	1.42	0.07	Pyrrhotite
7	1.61	35.02	66.32	1.89	0.05	1.61	35.02	66.32	1.43	0.05	Pyrrhotite
8	41.08	61.36	0.00	0.00	0.67	41.08	61.36	0.00	0.00	0.67	Iron Oxide
9	3.04	34.65	66.22	1.91	0.09	3.04	34.65	66.22	1.44	0.09	Pyrrhotite
10	45.83	56.06	6.77	0.12	0.82	45.83	56.06	6.77	0.12	0.82	Iron Oxide
11	43.01	60.38	0.72	0.01	0.71	43.01	60.38	0.72	0.01	0.71	Iron Oxide

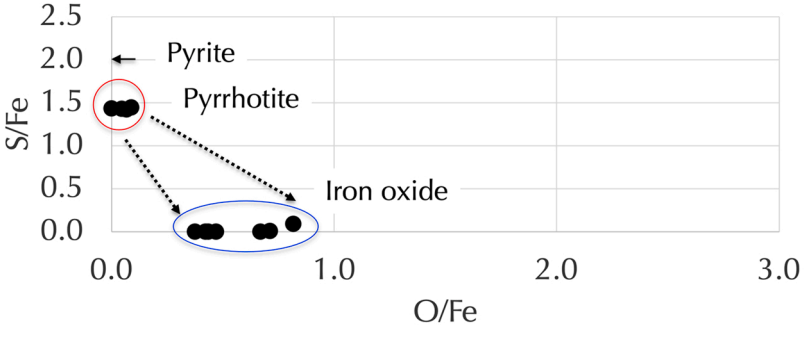

(caption on next page)

Fig. 11. Backscatter electron image (top) and X-ray compositional analyses of concrete showing compositions of oxidized iron veins within pyrrhotite measured at the tips of callouts that are provided in the Table below the image. Pyrrhotite shows typical high FeO and SO_3 whereas oxidized iron veins within pyrrhotite show mostly FeO.

polished cross sections and thin sections especially after impregnating the sections with a fluorescent dye-mixed low-viscosity epoxy and observing in an UV light.

Internal microcracks are often associated with reddish-brown iron oxide and hydroxide oxidation products and/or ettringite as deleterious reaction products whereas external manifestation of such cracks often bring those reaction products to the surface where upon atmospheric carbonation many sulfate and carbonate efflorescence deposits may preferentially form along the cracks.

4.7. Secondary ettringite from internal sulfate attacks

Petrographic examinations of distressed residential foundation in the present study, as well as from other distressed homes of eastern Connecticut, have detected abundant secondary ettringite crystallization lining or filling many air voids and occasionally lining some microcracks that are indicative of prolonged presence of moisture in concretes during service, which is an essential prerequisite for pyrrhotite oxidation. Presence of moisture also indicates availability of sulfates to be released from pyrrhotite-oxidation and for subsequent ettringite crystallization, which, however, may or may not have necessarily derived from pyrrhotite oxidation since ettringite-filled air-voids are a very common microstructural feature in a concrete exposed to moisture without even any iron sulfide contaminant. Any Portland cement concrete exposed to moisture during service forms secondary ettringite deposits lining and filling air voids. To establish the source of secondary ettringite i.e. from Portland cement's sulfate and/or from oxidation of pyrrhotite-bearing aggregates require determination of sulfate levels in concrete i.e. if the level is higher than that expected from a typical Portland cement concrete where sulfate (as SO_3) content in cement is around 3 wt percent i.e. giving about 0.45% sulfate in concrete for a usual cement content of 15% by mass of a normal weight concrete. Excess sulfate in concrete above 0.45% from cement's contribution would then correspond to the pyrrhotite-aggregate source if no other sulfate source were present. The present study showed 2.37% sulfate in concrete, i.e., significantly higher than the sulfate normally contributed from Portland cement due to contribution from pyrrhotite oxidation.

5. Discussions

Case studies on pyrrhotite-oxidation-related distress of concrete foundations from eastern Connecticut by the present and previous [2–4] studies have confirmed and provided clear mechanisms of the common consensus that the cracking and crumbling of many concrete foundation walls in eastern Connecticut are due to: (a) oxidation of pyrrhotite in crushed garnetiferous quartzo-feldspathic and biotite gneiss coarse aggregate particles *in the presence of oxygen and moisture during service* with formation of ferrihydrite causing expansion of the unsound aggregates and formation of cracks from unsound aggregates to paste, which was then followed by (b) additional expansions in the paste from reactions between sulfates released from pyrrhotite oxidation and cement hydration products (internal sulfate attack) and formation of poorly crystalline or perhaps colloidal ettringite within the confined spaces in paste.

Visible and invisible cracking in the concrete foundation and evidence of pyrrhotite-oxidation-related distress confirms: (a) the source of coarse aggregate of concrete in this case was possibly derived from the Becker's quarry, which has produced unsound aggregates for other distressed foundations [30], and, (b) the prolonged presence of moisture in the foundation during service. Cracking, high sulfate, and resultant sulfate products are similar to other types of concrete deteriorations, e.g., in chimney or sewer environments [31] or in the cases of delayed ettringite formation [32] but direct establishment of the source of high sulfate from pyrrhotite oxidation is crucial to differentiate this distress from others. Perhaps slow uptake of moisture through the wall from the ground level could have initiated pyrrhotite oxidation and resultant cracking, which is similar in other residential foundations of eastern Connecticut that have shown distress after 10–20 years since construction, the time period within which the present foundation reportedly falls.

6. Summary and conclusion

Extensive cracking of a residential concrete foundation in Mansfield, CT has not only confirmed the presence of disseminated pyrrhotite inclusions in crushed gneiss coarse aggregates, but also evidence of pyrrhotite-oxidation-related cracking and associated internal sulfate attack in the mortar fraction from the sulfates released by pyrrhotite oxidation. Crushed gneiss coarse aggregates are similar to the ones from other distressed foundations in having a greater proportion of dark gray and brown granite gneiss than the white gneiss where the former two gneiss types contained noticeable disseminated pyrrhotite inclusions as in other pyrrhotite-bearing dark gray and brown gneiss quarried from the hydrothermal vein of pyrrhotite crystallization in the Becker's quarry in Willington, CT that has provided the unsound aggregate for other distressed foundations. Extensive macro and micro cracking in foundations are testament of deleterious pyrrhotite oxidation. Very high sulfate (as SO_3) contents of concretes (as high as 2.7% SO_3) compared to 0.45% SO_3 in normal Portland cement concretes indicates additional sulfate sources beside Portland cement, which is confirmed to be from pyrrhotite in aggregates. XRD studies did not detect measurable pyrrhotite in concrete or even in extracted coarse aggregates (despite its detection from optical microscopy and SEM) but the oxidation product ferrihydrite is detected, which is in conformance to optical microscopy, SEM-EDS and other studies. SEM-EDS studies have detected veins of oxidized iron in iron sulfide bodies in pyrrhotite along with sulfate contamination in the paste from sulfates released from pyrrhotite oxidation. Optical microscopy and SEM-

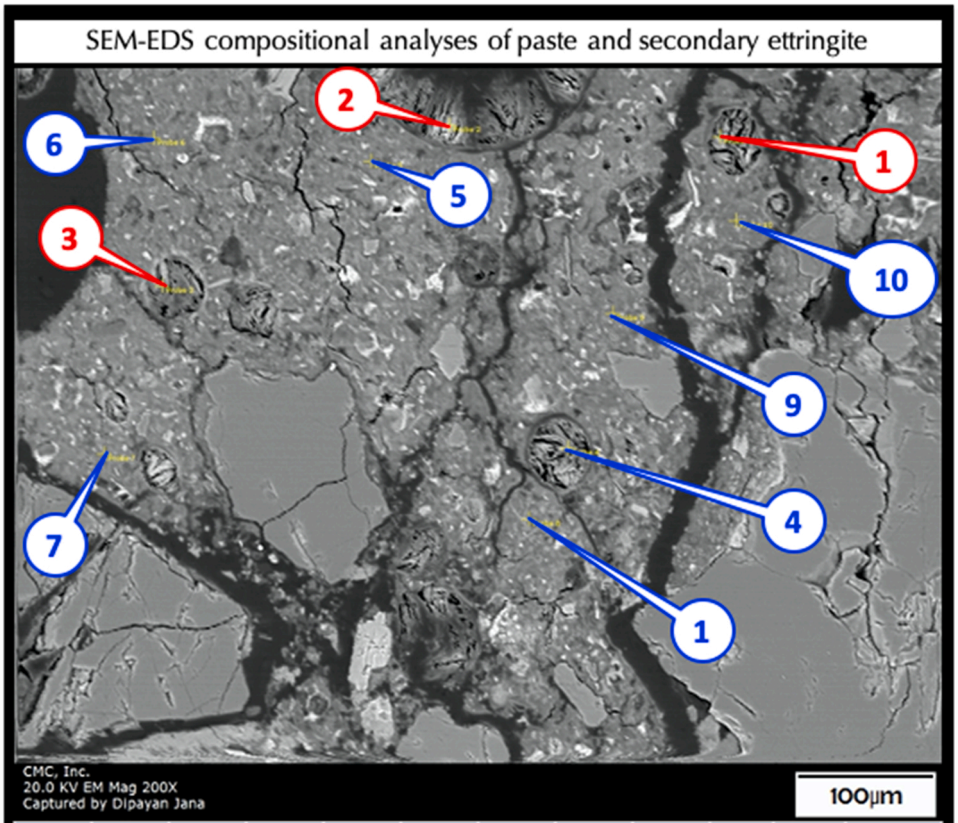

Probe	CaO	SiO_2	Al_2O_3	Na_2O	MgO	SO_3	K_2O	TiO_2	FeO	Total	Phase
1	68.98	9.24	9.52	0.01	0.00	11.80	0.45	0.01	0.01	100.02	Ettringite
2	61.01	11.42	13.10	0.01	0.00	11.56	0.30	0.11	2.49	100.00	Ettringite
3	60.32	7.84	15.94	0.01	0.01	12.43	0.00	2.14	1.31	100.00	Ettringite
4	63.27	6.07	11.52	0.01	0.04	16.40	0.66	0.01	2.02	100.00	Paste
5	61.12	32.02	0.84	0.01	0.01	0.01	0.01	0.46	5.52	100.00	Paste
6	56.44	33.12	2.88	0.02	0.01	0.01	0.01	0.72	6.80	100.01	Paste
7	57.05	34.08	1.57	0.02	0.01	0.01	0.18	2.46	4.63	100.01	Paste
8	53.16	33.02	4.15	0.01	0.01	0.00	0.00	0.01	9.63	99.99	Paste
9	56.83	27.85	5.04	0.02	0.24	0.53	0.25	0.01	9.23	100.00	Paste
10	48.00	38.51	6.39	0.01	0.48	0.01	1.99	0.13	4.49	100.01	Paste

Fig. 12. Backscatter electron image (top) and X-ray compositional analyses of concrete showing compositions of secondary ettringite deposits in voids and various areas of paste at the tips of callouts that are provided in the Table below the image. Secondary ettringite shows high Ca, Al, and S whereas paste shows typical calcium silicate hydrate composition with negligible or no evidence of contamination by sulfates released from pyrrhotite oxidation, which is typically found in many other pyrrhotite-related distress in the area.

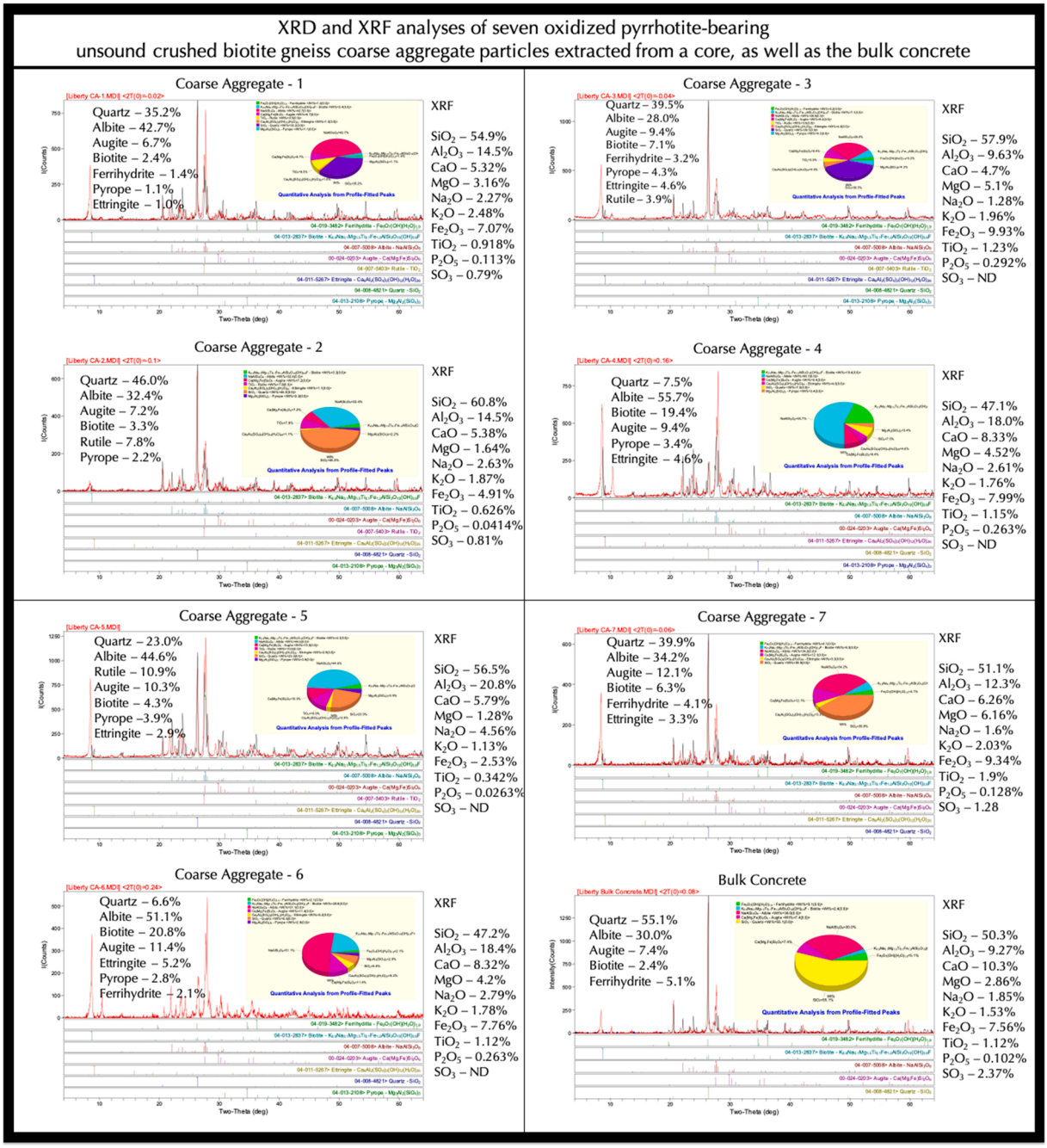

Fig. 13. Mineralogical and chemical evidence of pyrrhotite oxidation – detection of ferrihydrite as the oxidation product of pyrrhotite, and ettringite from the released sulfate from oxidation, along with the host mineralogies (e.g., quartz, feldspar, biotite, pyrope garnet, etc.) of coarse aggregates. Right columns show XRF results of the same aggregates and of bulk concrete, where high levels of sulfate are detected in some aggregates and especially in the bulk concrete beyond cement's contribution to indicate additional sulfate released from pyrrhotite oxidation. Inset pie charts in XRD show relative proportions of various phases detected from Rietveld analysis.

EDS studies both detected many deleterious secondary ettringite formation in paste, voids, and cracks, which (along with high total sulfate in concretes) are testament of additional sulfate sources beyond cement, from pyrrhotite with expansion and cracking from pyrrhotite oxidation. Ion chromatography of crushed gneiss coarse aggregates extracted from concrete showed potential release of sulfate in a highly oxidizing solution of hydrogen peroxide, indicating a similar potential release of sulfate in the field in prolonged oxidizing condition from the presence of moisture. This indicates role of prolonged presence of moisture and moisture penetration through existing cracks in foundations to sustain pyrrhotite oxidation and continued distress.

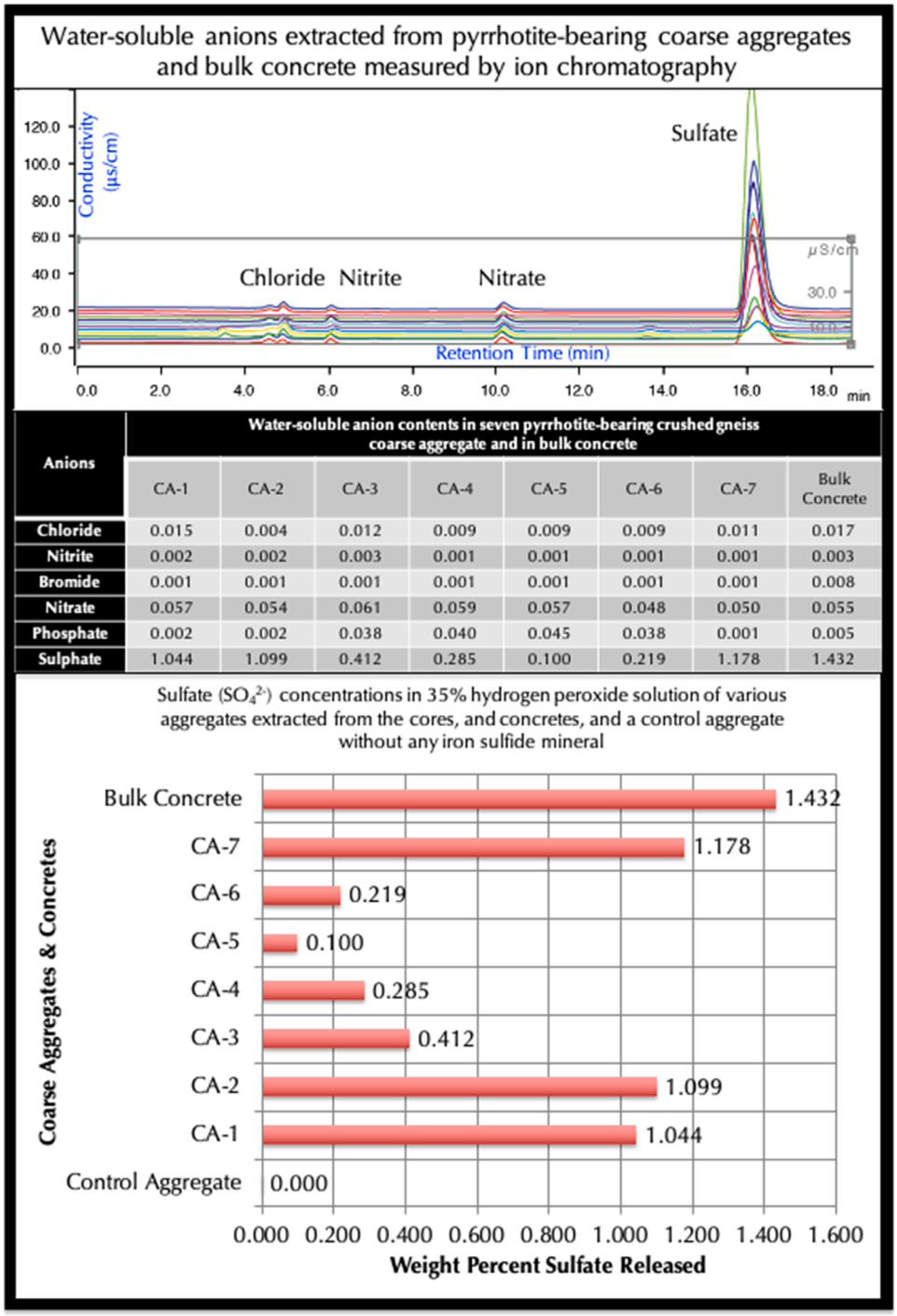

Anions	Water-soluble anion contents in seven pyrrhotite-bearing crushed gneiss coarse aggregate and in bulk concrete							
	CA-1	CA-2	CA-3	CA-4	CA-5	CA-6	CA-7	Bulk Concrete
Chloride	0.015	0.004	0.012	0.009	0.009	0.009	0.011	0.017
Nitrite	0.002	0.002	0.003	0.001	0.001	0.001	0.001	0.003
Bromide	0.001	0.001	0.001	0.001	0.001	0.001	0.001	0.008
Nitrate	0.057	0.054	0.061	0.059	0.057	0.048	0.050	0.055
Phosphate	0.002	0.002	0.038	0.040	0.045	0.038	0.001	0.005
Sulphate	1.044	1.099	0.412	0.285	0.100	0.219	1.178	1.432

Fig. 14. Accelerated oxidation tests of seven crushed gneiss coarse aggregate particles extracted from the concrete core, along with the pulverized concrete after digestion in hydrogen peroxide solutions for 10 days to determine various levels of sulfates released from oxidation. All show noticeable release of sulfate, especially the concrete itself compared to a control aggregate with no iron sulfide inclusion. The top graph shows superposed anion chromatograms of all samples.

A recent map (Fig. 1) of potential pyrrhotite-bearing rocks across continental US compiled by USGS shows a narrow elongated belt of intense pyrrhotite crystallization along the metamorphic rocks of the Appalachian mountain range along eastern US, which poses a serious threat of potential incorporation of these rocks in concrete, and related distress at least in the states of Connecticut and Massachusetts where more than 35,000 homes are already affected.

Unfortunately, there is no standardized test to detect the presence and amount of potentially deleterious pyrrhotite in aggregates, which should be screened by a five-phase testing protocol [4] starting with (a) detailed petrographic examinations from stereomicroscopical examinations of lapped cross sections to examinations of thin sections in reflected-light (ore) microscope and transmitted polarized light microscopes and further SEM-EDS studies to detect the presence of pyrrhotite, (b) total sulfur contents of aggregates from all sulfide and sulfate phases determined by XRF or combustion IR method with a threshold limit of 0.1% maximum total sulfur by mass for acceptance, above which for the aggregates having sulfur contents in the range of 0.1% and 1% requires additional tests of (c) XRD or magnetic susceptibility drop across the curie temperature (325 °C, [33]) to determine the amount of pyrrhotite in the sulfide phases, and XRD to identify and quantify the oxidation products of pyrrhotite, (d) accelerated oxidation [2,4] or oxygen consumption [34] test of pulverized aggregates to determine the potential to release sulfates, and, (e) accelerated mortar bar expansion test of laboratory-cured mortar or concrete prisms with the suspected aggregates (which showed >5% oxygen consumption) for potentially deleterious (> 0.1%) expansion in the presence of oxygen and moisture [35].

Funding

This research did not receive any specific grant from funding agencies in the public, commercial, or not-for-profit sectors.

Declaration of Competing Interest

The authors declare that they have no known competing financial interests or personal relationships that could have appeared to influence the work reported in this paper.

References

[1] W.A. Deer, R.A. Howie, J. Zussman. An Introduction to the Rock-Forming Minerals, third ed., Berforts Information Press, UK, 2013, p. 696.
[2] K. Wille, R. Zhong, Investigating the Deterioration of Basement Walls Made of Concrete in CT, University of Connecticut, Storrs, CT, 2016.
[3] R. Zhang, K. Wille, Deterioration of residential concrete foundations: the role of pyrrhotite-bearing aggregate, Cem. Concr. Compos. 94 (2018) 53–61.
[4] D. Jana, Pyrrhotite epidemic in Easternal Connecticut: diagnosis and prevention, Acids Mater. J. 117 (1) (2020) 1–20.
[5] J. Moum, I.Th Rosenqvist, Sulfate attack on concrete in the Oslo region, J. Am. Concr. Inst. 56 (18) (1959) 257–264.
[6] A. Tagnit-Hamou, M. Saric-Coric, P. Rivard, Internal deterioration of concrete by oxidation of pyrrhotitic aggreates, Cem. Concr. Res. 35 (2005) 99–107.
[7] A. Rodrigues, J. Duchesne, B. Fournier, Mineralogical and chemical assessment of concrete damaged by oxidation of sulphide-bearing aggregates, Cem. Concr. Res. 42 (2012) 1336–1347.
[8] J. Duchesne, F. Benoit, Deterioration of concrete by the oxidation of sulphide minerals in the aggregate, J. Civ. Eng. Archit. 7 (8) (2013) 922–931.
[9] J. Duchesne, B. Fournier, Petrography of concrete deteriorated by weathering of sulphide minerals, in: Proceedings of the International Cement Microscopy Association Conference, April 2011.
[10] G.S. Araujo, J.S. Chinchon, A. Aguado, Evaluation of the behavior of concrete gravity dams suffering from internal sulfate attack, IBRACON Struct. Mater. J. 1 (1) (2008) 84–112.
[11] J.S. Chinchon, C. Ayora, A. Aguado, F. Guirado, Influence of weathering of iron sulfides contained in aggregates on concrete durability, Cem. Concr. Res. 25 (6) (1995) 1264–1272.
[12] S. Chinchon-Paya, A. Aguado, S. Chinchon, A comparative investigation of the degradation of pyrite and pyrrhotite under simulated laboratory conditions, Eng. Geol. 127 (2012) 75–80.
[13] C. Ayora, J.S. Chinchon, A. Aguado, F. Guirado, Weathering of iron sulfides and concrete alteration: thermodynamic model and observation in dams from Central Pyrenees, Spain, Cem. Concr. Res. 28 (4) (1998) 1223–1235.
[14] I. Oliveira, S.H.P. Cavalaro, A. Arguado, Evolution of pyrrhotite oxidation in aggregates for concrete, Mater. Constr., 038(64), 2104, p. 316.
[15] R.M. Quigley, R.W. Vogan, Black shale heaving at Ottawa, Canada, Can. Geotech. J. 7 (2) (1970) 106–112.
[16] J. Berard, Black shale heaving at Ottawa, Canada: Discussion, Can. Geotech. J. (1970) 113–114.
[17] M.A. Berube, J. Locat, P. Gelinas, J.Y. Chagon, P. Lefrancois, Heaving of black shale in Quebec City, Can. J. Earth Sci. 23 (1986) 1774–1781.
[18] E. Penner, W.J. Eden, W.J. Grattan-Bellew, Expansion of Pyritic Shales, NRC Publication Archive, Canadian Building Digest, CBD, Vol. 152, 1972.
[19] A.B. Hawkins, G.M. Pinches, Cause and significance of heave at Llandough Hospital, Cardiff – a case history of ground floor heave due to gypsum growth, Q. J. Eng. Geol. Hydrogeol. 20 (1987) 41–57.
[20] S.E. Hoover, D. Lehmann, The expansive effects of concentrated pyritic zones within the Devonian Marcellus Shale formation of North America, Q. J. Eng. Geol. Hydrogeol. 42 (2) (2009) 157–164.
[21] W.H. Anderson, Foundation Problems and Pyrite Oxidation in the Chattanooga Shale, Geological Survey Report of Investigation, Estill County, Kentucky: Kentucky Geological Survey, Series XII, Report of Investigations 18, 2008.
[22] A. Shayan, Deterioration of a concrete surface due to the oxidation of pyrite contained in pyritic aggregate, Cem. Concr. Res. 18 (5) (1988) 723–730.
[23] M.L. Jeffrey, New USGS Map Helps Identify Where Pyrrhotite, A Mineral That Can Cause Concrete Foundations to Fail, May Occur, United States Geological Survey, 2020. ⟨https://www.usgs.gov/news/new-usgs-map-helps-identify-where-pyrrhotite-a-mineral-can-cause-concrete-foundations-fail-may⟩.
[24] J. Gourley, Trinity College Environmental Science Program, Hartford, CT, and Margaret Thomas CT State Geologist, 2018.
[25] ASTM C 856 Standard Practice for Petrographic Examination of Hardened Concrete, West Conshohocken, PA, ASTM International, Vol. 4.02, 2014.
[26] ASTM C 1723 Standard Guide for Examination of Hardened Concrete Using Scanning Electron Microscopy, West Conshohocken, PA, ASTM International, 2016.
[27] ASTM C 1365 Standard Test Method for Determination of the Proportion of Phases in Portland Cement and Portland-Cement Clinker Using X-Ray Powder Diffraction Analysis, West Conshohocken, PA, ASTM International, 2018.
[28] ASTM D 4327 Standard Test Method for Anions in Water by Suppressed Ion Chromatography, West Conshohocken, PA, ASTM International, 2017.
[29] A. Rodrigues, J. Duchesne, B. Fournier, Quantitative assessment of the oxidation potential of sulfide-bearing aggregates in concrete using an oxygen consumption test, Cem. Concr. Compos. 67 (2016) 93–100.
[30] S.J. O'Neill, Pyrrhotite Contaminated Concrete – A Call for Collaboration, AIA Western Massachusetts Newsletter, 2018, pp. 11–14.
[31] D. Jana, Concrete deterioration from pyrite staining, sewer gases, and chimney flue gases – case studies showing microstructural similarities, in: Proceedings of the 30th Conference on Cement Microscopy, ICMA, Reno, Nevada, 2008.
[32] D. Jana, DEF and ASR in concrete – a systematic approach from petrography, in: Proceedings of the 30th Conference on Cement Microscopy, ICMA, Reno, Nevada, 2008.

[33] C.E. Geiss, J.R. Gourley, A thermomagnetic technique to quantify the risk of internal sulfur attack due to pyrrhotite, Cem. Concr. Res. 115 (2019) 1–7.
[34] A. Rodrigues, J. Duchesne, B. Fournier, Quantitative assessment of the oxidation potential of sulfide-bearing aggregates in concrete using an oxygen consumption test, Cem. Concr. Compos. 67 (2016) 93–100.
[35] A. Rodrigues, J. Duchesne, B. Fournier, A new accelerated mortar bar test to assess the potential deleterious effect of sulfide-bearing aggregate in concrete, Cem. Concr. Res. 73 (2015) 96–110.